

Supporting Information for A Classical Polarizable Force Field for Clays: Pyrophyllite and Talc

Stéphane Tesson, Mathieu Salanne, Benjamin Rotenberg, Sami Tazi, and
Virginie Marry*

Sorbonne Universités, UPMC Univ Paris 06, CNRS, Laboratoire PHENIX, Case 51, 4

Place Jussieu, F-75005 Paris, France

E-mail: virginie.marry@upmc.fr

Phone: +33 (0)1 44272203

Sheets structure details

Table S1: Average bond lengths and angles for pyrophyllite. The relative difference between experimental and simulation results (in percent) is given in parenthesis. The standard errors (SE) are calculated by the error block averaging method.^{1,2} The SE, which apply on the last digit of the given values, are estimated to be 4 and 8 for the distances and the angles respectively.

Pyrophyllite	PIM	ClayFF	Exp. ³
<u>Tetrahedra</u>			
Bond lengths (\AA)			
Si-O _a	1.63 (0.2)	1.64 (0.1)	1.63
Si-O _b	1.62 (0.6)	1.57 (2.9)	1.61
O _a -O _a	3.03 (0.7)	3.02 (0.4)	3.01
O _a -O _b	2.67 (0.6)	2.55 (3.9)	2.65
O _b -O _b	2.69 (1.9)	2.61 (1.0)	2.63
Angles ($^\circ$)			
O _a -Si-O _b (1 or 3)	108.1 (0.5)	105.7 (2.7)	108.7
O _a -Si-O _b (2)	110.5 (0.0)	110.8 (0.3)	110.5
O _b -Si-O _b	109.3 (0.3)	112.9 (3.0)	109.6
Si(1)-O _b (1 or 3)-Si(2)	130.5 (0.9)	143.7 (9.2)	131.7
Si(1)-O _b (2)-Si(2)	140.1 (3.2)	144.7 (0.0)	144.7
<u>Octahedra</u>			
Bond lengths (\AA)			
Al-O _a	1.97 (2.2)	2.00 (3.8)	1.92
Al-O _{OH}	1.85 (2.1)	2.00 (6.0)	1.89
O _a (1)-O _a (2 or (1) ^b)	2.81 (1.0)	2.85 (2.7)	2.78
O _a (2) ^b -O _a (2 or (1) ^b)			
O _{OH} -O _a (1, (1) ^b or 2)	2.66 (5.2)	3.10 (10.4)	2.80
O _{OH} ^b -O _a ((1) ^b , (2) or (2) ^b)			
O _a (1)-O _a (2) ^b	2.92 (0.6)	2.70 (7.9)	2.93
O _{OH} -O _{OH} ^b	2.30 (1.8)	2.63 (12.3)	2.34
Angles ($^\circ$)			
O _a (1)-Al-O _a ((1) ^b or 2)	94.3 (0.5)	94.6 (0.1)	94.8
O _a (2) ^b -Al-O _a ((1) ^b or 2)			
O _{OH} (1)-Al-O _a ((1) ^b or 2)	96.6 (0.8)	97.2 (1.5)	95.8
O _{OH} (2) ^b -Al-O _a ((1) ^b or 2)			
O _a (1)-Al-O _{OH}	93.4 (0.7)	92.3 (0.5)	92.7
O _a (2) ^b -Al-O _{OH} ^b			
O _a (1)-Al-O _a (1) ^b	78.0 (0.2)	86.2 (10.8)	77.8
O _a (2)-Al-O _a (2) ^b			
O _{OH} -Al-O _{OH} ^b	77.7 (1.5)	84.8 (10.8)	76.5

Table S2: Average bond lengths and angles for talc. The relative difference between experimental and simulation results (in percent) is given in parenthesis. The standard errors (SE) are calculated by the error block averaging method.^{1,2} The SE, which apply on the last digit of the given values, are estimated to be 4 and 8 for the distances and the angles respectively.

Talc	PIM	ClayFF	Exp. ⁴
<u>Tedrahedra</u>			
Bond lengths (\AA)			
Si-O _a	1.63 (0.4)	1.58 (2.3)	1.62
Si-O _b	1.63 (0.3)	1.58 (2.7)	1.62
O _a -O _a	3.01 (-)	3.06 (-)	-
O _a -O _b	2.67 (-)	2.67 (-)	-
O _b -O _b	2.69 (-)	2.63 (-)	-
Angles ($^\circ$)			
O _a -Si-O _b (1 or 3)	108.3 (0.7)	108.9 (0.2)	109.1
O _a -Si-O _b (2)	110.2 (0.8)	110.3 (0.9)	109.4
O _b -Si-O _b	109.0 (0.7)	112.1 (2.1)	109.8
Si(1)-O _b (1 or 3)-Si(2)	130.8 (-)	143.6 (-)	-
Si(1)-O _b (2)-Si(2)	140.5 (-)	144.5 (-)	-
<u>Octahedra</u>			
Bond lengths (\AA)			
Mg-O _a	2.06 (0.8)	2.10 (1.0)	2.08
Mg-O _{OH}	2.06 (0.0)	2.19 (6.3)	2.06
O _a (1)-O _a (2 or (1) ^b)	2.77 (5.4)	2.75 (5.9)	2.92
O _a (2) ^b -O _a (2 or (1) ^b)			
O _{OH} -O _a (1, (1) ^b or 2)	3.02 (2.9)	3.12 (6.3)	2.93
O _{OH} ^b -O _a ((1) ^b , (2) or (2) ^b)			
O _a (1)-O _a (2) ^b	2.75 (0.1)	2.69 (2.2)	2.75
O _{OH} -O _{OH} ^b	2.80 (1.3)	2.75 (0.2)	2.76
Angles ($^\circ$)			
O _a (1)-Mg-O _a ((1) ^b or 2)	94.5 (0.1)	91.7 (2.9)	94.5
O _a (2) ^b -Mg-O _a ((1) ^b or 2)			
O _{OH} (1)-Mg-O _a ((1) ^b or 2)	97.7 (2.4)	92.0 (3.6)	95.4
O _{OH} (2) ^b -Mg-O _a ((1) ^b or 2)			
O _a (1)-Mg-O _{OH}	93.3 (1.8)	91.3 (4.0)	95.0
O _a (2) ^b -Mg-O _{OH} ^b			
O _a (1)-Mg-O _a (1) ^b	78.2 (8.5)	90.5 (6.0)	85.5
O _a (2)-Mg-O _a (2) ^b			
O _{OH} -Mg-O _{OH} ^b	77.4 (8.0)	90.2 (7.3)	84.1

DFT

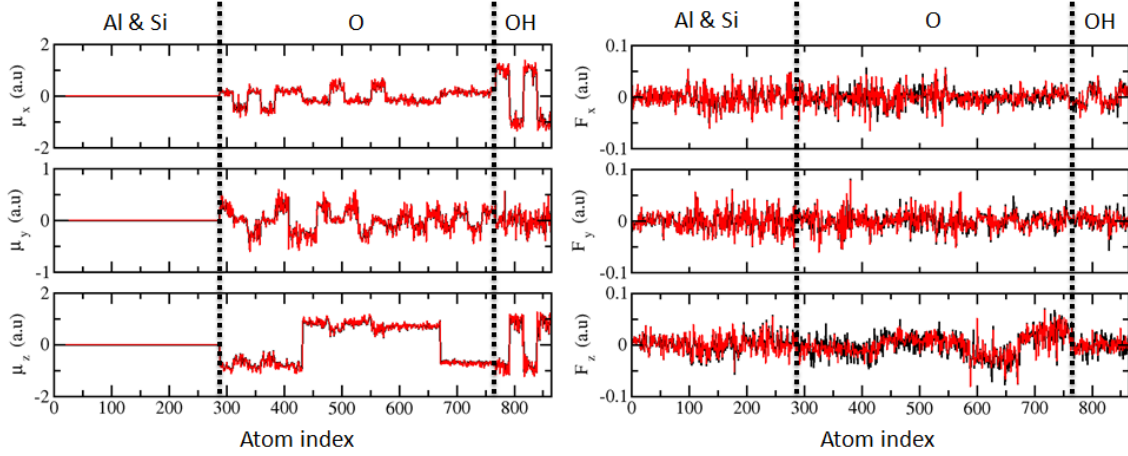


Figure S1: Dipoles (left) and Forces (right) on each atom for one of the pyrophyllite configurations. The predictions of the BLYP functional with DZVP plane-wave basis set (black lines) for the dipole components (μ_x , μ_y and μ_z) and the force components (F_x , F_y and F_z) are compared to that of the the PBE functional with DZVP plane-wave basis set (red lines).

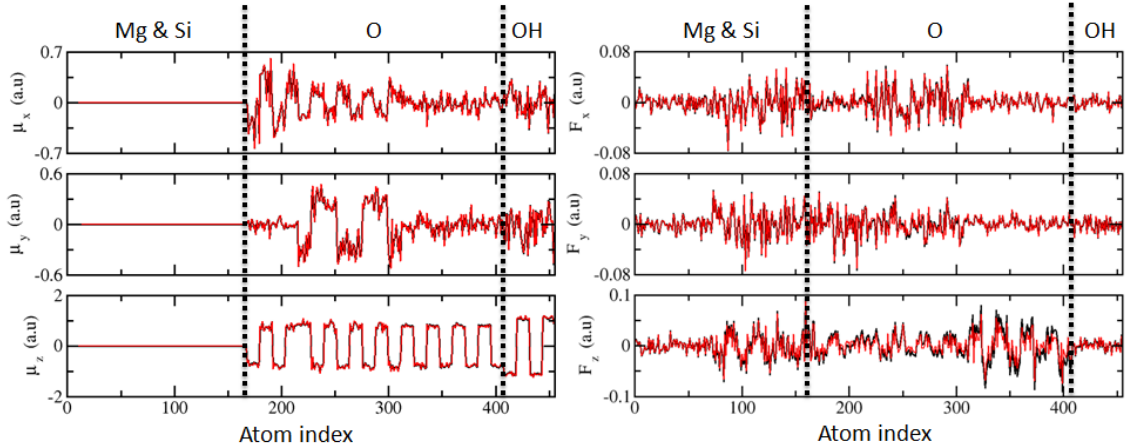


Figure S2: Dipoles (left) and Forces (right) on each atom for one of the talc configurations. The predictions of the PBE functional with DZVP plane-wave basis set (black lines) for the dipole components (μ_x , μ_y and μ_z) and the force components (F_x , F_y and F_z) are compared to that of the PBE functional with TZV2P plane-wave base set (red lines).

ClayFF force field

The ClayFF force field for pyrophyllite and talc is described in Table S3. Lorentz-Berthelot mixing rules are used to determine the cross-parameters ϵ_{ij} and σ_{ij} .

Table S3: Parameters of the ClayFF force field.⁵

Systems	Atoms	Symbols	ϵ (kJ.mol ⁻¹)	σ (Å)	Charge (e)
Pyrophyllite	Si	st	7.700652 10 ⁻⁶	3.302027	+2.1000
	Al	ao	5.563883 10 ⁻⁶	4.271236	+1.5750
	O _b	ob	6.501936 10 ⁻¹	3.165541	-1.0500
	O _a	oa	6.501936 10 ⁻¹	3.165541	-1.0500
	O _{OH}	oh	6.501936 10 ⁻¹	3.165541	-0.9500
	H	ho	-	-	+0.4250
Talc	Si	st	7.700652 10 ⁻⁶	3.302027	+2.1000
	Mg	mgo	3.778068 10 ⁻⁶	5.264321	+1.3600
	O _b	ob	6.501936 10 ⁻¹	3.165541	-1.0500
	O _a	oa	6.501936 10 ⁻¹	3.165541	-1.2825
	O _{OH}	oh	6.501936 10 ⁻¹	3.165541	-0.9500
	H	ho	-	-	+0.4250

References

- (1) Frenkel, D.; Smit, D. Understanding Molecular Simulations: from Algorithms to Applications. In *Academic Press*, Vol. 1; Frenkel, D.; Smit, D., Eds.; Academic Press, 2001; pp 98–105.
- (2) Flyvbjerg, H.; and Petersen, H. G. Error estimates on averages of correlated data. *J. Chem. Phys.* **1989**, *91*, 461–466.
- (3) Lee, J. H.; Guggenheim, S. Single crystal X-ray refinement of pyrophyllite-1Tc. *Am. Mineral.* **1981**, *66*, 350–357.

- (4) Rayner, J. H. The crystal structure of talc. *Clay Clay Miner.* **1973**, *21*, 103–114.
- (5) Cygan, R.; Liang, J.-J.; Kalinichev, A. Molecular models of hydroxide, oxyhydroxide, and clay phases and the development of a general force field. *J. Phys. Chem. B* **2004**, *108*, 1255–1266.